Cosmic Evolution of Active Galactic Nuclei

Jacobo Ebrero and Francisco J. Carrera

Abstract The X-ray Luminosity Function (XLF) is a key tool to understand the evolution of Active Galactic Nuclei (AGN) and the variation in the accretion rate of matter onto the supermassive black hole that resides in their centres along cosmic time. We have studied the density of sources per unit luminosity in three energy bands combining the XMS survey with other shallower and deeper samples, up to redshifts of $\sim$3. The XMS survey covers a sky area of $\sim$3.3 sq. degrees at medium fluxes, where the bulk of the Cosmic X-ray Background is emitted. Moreover, extragalactic surveys such as XMS are essential since they contain a large amount of obscured AGN that decisively contribute to the background emission. We have found evolution in the AGN detected in soft (0.5-2 keV), hard (2-10 keV) and ultrahard (4.5-7.5 keV) X-rays, finding a maximum in the comoving density of these objects at redshifts of $\sim$1. Since we have detailed spectral information of most of the AGN detected at $>$2 keV, we have studied their XLF along with their instrinsic absorption properties in order to obtain purely observational results and to determine the evolution of absorbed AGN at different epochs of the Universe.

1 Introduction

One of the main goals of X-ray surveys is to study the cosmological properties of Active Galactic Nuclei (AGN) as they are strongly linked to the accretion history of the Universe and the formation and growth of the supermassive black holes that are believed to reside in the centre of all galaxies, active or not. The first studies in

J. Ebrero
Instituto de Física de Cantabria (CSIC-UC), Avenida de Los Castros, 39005 Santander (Spain), e-mail: ecarrero@ifca.unican.es

F. J. Carrera
Instituto de Física de Cantabria (CSIC-UC), Avenida de Los Catros, 39005 Santander (Spain) e-mail: carreraf@ifca.unican.es

this field were constrained to the soft X-ray band ($\leq$2 keV) which could be biased against absorbed AGN. Therefore, hard X-ray surveys ($>$2 keV) are essential to describe the luminosity function of the entire AGN population, including obscured AGN which are the main contributors to the cosmic X-ray background.

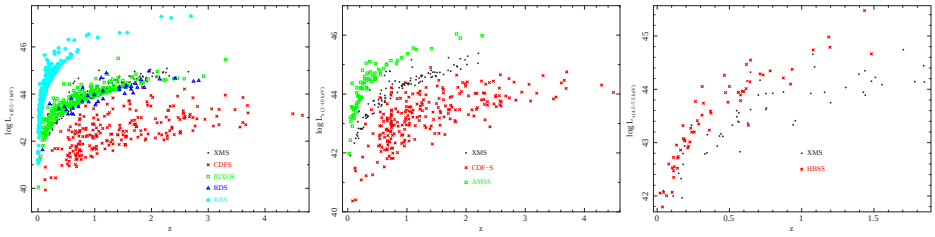

Fig. 1 Luminosity-redshift plane of different X-ray surveys in the Soft (*Left panel*), Hard (*Center panel*) and Ultrahard (*Right panel*) bands.

In this work we use the *XMM-Newton* Medium Survey (XMS, [2]), along with other highly complete deeper and shallower surveys, to compute the X-ray luminosity function in several energy bands. Furthermore, given the availability of high-quality X-ray spectral information in the XMS, we are able to model the intrinsic absorption of the sources detected above 2 keV as a function of the X-ray luminosity up to column densities of $\sim 10^{24}$ cm^{-2}. These issues are key tools to probe the accretion history of the Universe across cosmic time. Thanks to the extremely high identification completeness of the XMS sample and the accompanying surveys we have assembled an overall sample of $\sim$1000 identified AGN in the 0.5-2 keV, $\sim$450 identified AGN in the 2-10 keV band, and $\sim$120 identified AGN in the 4.5-7.5 keV bands, leading to one of the largest and most complete sample up to date in all three energy bands.

Throughout this work we have assumed a cosmological framework with $H_0 = 70$ km s^{-1} Mpc^{-1}, $\Omega_M = 0.3$ and $\Omega_\Lambda = 0.7$ (Spergel at al. [15]).

2 The X-ray data

The backbone of the work presented in this paper is the XMS sample ([2]). This survey has typical exposure times of about 15 ks and hence is a medium survey, but in order to cover a wide luminosity and redshift range it is imperative to combine it with other complementary shallower and deeper surveys. Shallower, wider area surveys will provide significant numbers of bright sources at low redshifts, while deep pencil-beam surveys will probe fainter sources at greater distances.

Since the XMS survey is composed of different subsamples selected in several energy bands, we need to incorporate additional surveys on each of them. In the analysis performed in this paper we have used three energy bands defined as follows: Soft (0.5-2 keV), Hard (2-10 keV) and Ultrahard (4.5-7.5 keV).

Table 1 Summary of surveys used in this work, along with their flux limits, sky coverage, identification completeness and the number of identified AGN for each energy band.

Soft (0.5-2 keV)				
Survey	Flux limit (erg cm^{-2} s^{-1})	Area (deg^2)	Completeness (%)	N_{AGN}
RBS	2.5×10^{-12}	20300	100	310
RIXOS8	8.4×10^{-14}	4.44	100	40
RIXOS3	3.0×10^{-14}	15.77	94	182
XMS	1.5×10^{-14}	3.33	96	178
RDS	5.5×10^{-15}	0.30	92	39
CDF-S	5.5×10^{-17}	0.12	100[a]	226
Hard (2-10 keV)				
Survey	Flux limit (erg cm^{-2} s^{-1})	Area (deg^2)	Completeness (%)	N_{AGN}
AMSS	3.0×10^{-13}	68	99	79
XMS	3.3×10^{-14}	3.33	84	120
CDF-S	4.5×10^{-16}	0.11	100[a]	236
Ultrahard (4.5-7.5 keV)				
Survey	Flux limit (erg cm^{-2} s^{-1})	Area (deg^2)	Completeness (%)	N_{AGN}
HBSS	7.0×10^{-14}	25.17	97	62
XMS	6.8×10^{-15}	3.33	86	57

[a] Including photometric redshifts (see text).

All the surveys used in this work are summarized in Table 1. Apart from the XMS survey, we have used the CDF-S ([5]), RIXOS ([11]), RBS ([13]) and RDS ([7]) in the soft band; CDF-S and AMSS ([1]) in the hard band, and the HBSS ([3]) in the ultrahard band. They are all well-defined flux-limited surveys with very high identification completenesses, taken from already published catalogues of sources from diverse past and present X-ray observatories (*XMM-Newton*, *Chandra*, *ASCA*, *ROSAT*). In order to have an optimal $L_X - z$ plane coverage (see Figure 1), we will constrain our analysis to those sources identified as AGN with redshifts in the range $0.01 < z < 3$ in the Soft and Hard bands (spanning up to seven and six orders of magnitude in luminosity, respectively), and $0.01 < z < 2$ in the Ultrahard band (spanning up to four orders of magnitude in luminosity), being the vast majority of them spectroscopical redshifts. For the purposes of this work we have used the entire AGN population available (within the redshift limits stated above) irrespective of whether they were optically identified as Type-1 or Type-2 AGN. For the analysis in the hard and ultrahard bands we have also used the intrinsic absoption of the individual sources N_H when available.

3 The N_H function

Since hard X-ray photons are less affected by absorption, absorbed AGN are more likely to be detected at energies above 2 keV and hence we have studied their ab-

sorption properties in the Hard (2-10 keV) and Ultrahard (4.5-7.5 keV) sources, for which we have detailed spectral data (photon index Γ and intrinsic absorbing column densities N_H).

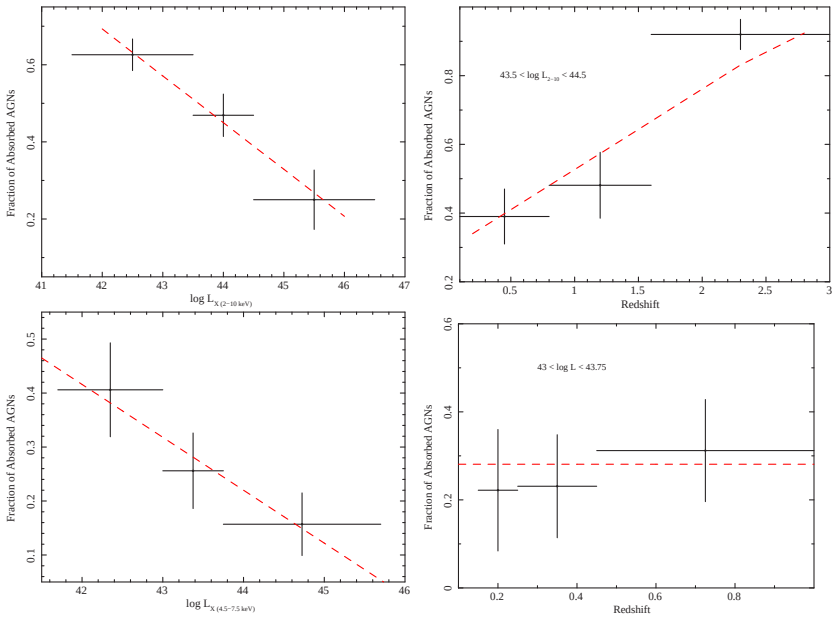

Fig. 2 Fraction of absorbed AGN as a function of the 2-10 (*Top left*) and 4.5-7.5 keV luminosity (*Bottom left*),and fraction of absorbed AGN as a function of redshift in the hard (*Top right*) and ultrahard (*Bottom right*) bands. Dashed lines represent the best-fit model of the N_H function using $N_H = 10^{22}$ cm^{-2} as the dividing value between obscured and unobscured AGN.

The N_H function is a probability distribution function for the absorption column density as a function of the X-ray luminosity and redshift. It is measured in units of $(\log N_H)^{-1}$ and is normalized to unity over the $\log N_H = 20 - 24$ region. The observed fraction of absorbed AGN (those with $\log N_H > 22$) is measured by the parameter ψ, which is generally function of both luminosity and redshift. Ccomparing the value of ψ in different luminosity ranges we can observe that the fraction of absorbed AGN is not constant, decreasing as the luminosity increases in both the Hard and Ultrahard bands. On the other hand, there is not significant variation in the value of ψ with redshift at a given luminosity in the Ultrahard band, which can be partly explained by the poor coverage in redshift of this sample, but there is a clear increase in the case of the Hard band (see Figure 2). Therefore, we will assume that the expression of ψ is dependent on both the X-ray luminosity and redshift and hence we have formalized its parametrization as a linear function of $\log L_X$ and z, similarly as in [9].

4 The X-ray luminosity function

In this section we will calculate the X-ray luminosity function (XLF) of our sources in the Soft, Hard and Ultrahard bands. The differential XLF measures the number of AGN per unit of comoving volume V and $\log L_X$, and is function of both luminosity and redshift and it is assumed that is a continous function over the luminosity and redshift ranges over which it is defined.

As shown in many works in the Soft and Hard bands ([12], [16], [8], [14]), the XLF seems to be best described as a double power law modified by a factor for evolution. We have implemented a Luminosity-dependent Density Evolution (LDDE) model in which the evolution factor not only depends on the redshift but also on the luminosity. We have fitted our sample to this model and to a Pure Luminosity Evolution (PLE) model using a Maximum Likelihood (ML) method ([10]), convolving it with the best-fit N_H function in the hard and ultrahard bands in order to take into account the instrinsic absoption properties of these sources. Best fit results from the XLF are shown in Figure 3.

5 Conclusions

We have discussed here the cosmic evolution of a sample of AGN in three X-ray bands: Soft (0.5-2 keV), Hard (2-10 keV) and Ultrahard (4.5-7.5 keV). The backbone of our sample is the XMS survey ([2]) which is a flux-limited highly-complete sample at medium redshifts. We have combined the XMS with other shallower and wider highly complete X-ray surveys in all three bands to end up with a total sample of $\sim$1000, 435 and 119 AGN in the Soft, Hard and Ultrahard bands, respectively.

We have used the detailed spectral information on the sources that compose the Ultrahard sample, XMS and HBSS to model their instrinsic absorption (N_H function). We find that the fraction of absorbed of AGN in the 4.5-7.5 keV band, assuming a dividing value of $N_H = 10^{22}$ cm^{-2}, is dependent on the X-ray luminosity but not on the redshift. This could be motivated by the narrow redshift range spanned by the sample, with the bulk of the sources located at low redshifts ($z < 1$). The same analysis applied to the Hard (2-10 keV) sources reveals dependency on both the X-ray luminosity and redshift. Our predictions on the behaviour of the fraction of absorbed AGN in this band is in excellent agreement with the results of [16] and [9] and with the more recent work of [6], who studied the evolution of the absorption properties of AGN in a compiled sample of 1290 AGN in the 2-10 keV band.

The best-fit XLF parameters in the Soft sample show slight discrepancies in both the overall shape and evolution with respect previous works in that band ([12], [8]). In the Hard band, where we have computed the intrinsic XLF taking into account the intrinsic absorption N_H of each source, we are in good agreement with the results of [16], [9] or [14]. Our best-fit model shows weaker evolution of the AGN below the cut-off redshift than in these works albeit with smaller error bars. In the Ultrahard band, we have also calculated the intrinsic XLF finding similar results as in [4]

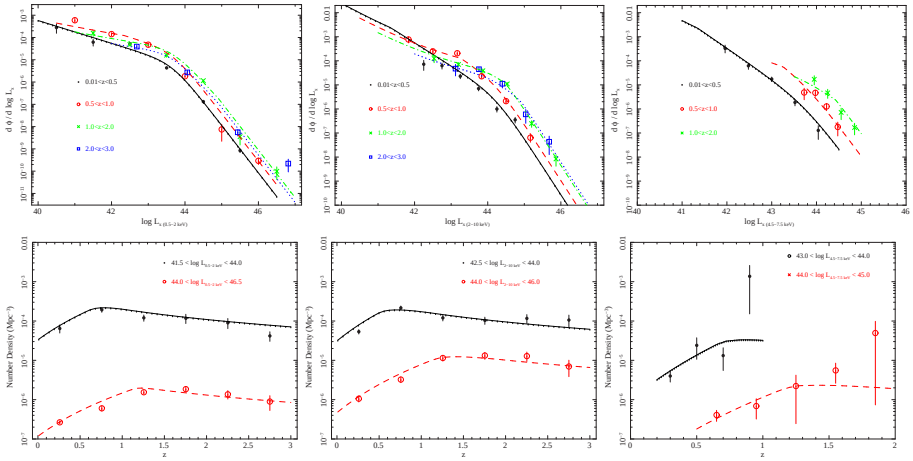

Fig. 3 Luminosity function of AGN in the Soft (*Top Left*), Hard (*Top Center*) and Ultrahard (*Top Right*) bands (overplotted are the best-fit XLF LDDE model for each redshift shell), and comoving density of AGN as a function of redshift in the Soft (*Bottom Left*), Hard (*Bottom Center*) and Ultrahard (*Bottom Right*) bands (overplotted are the best-fit XLF LDDE model predictions for each luminosity shell).

but with our best-fit parameters much more constrained. The results in this band show that Ultrahard AGN present a significantly stronger evolution below the cut-off redshift than those detected at softer energies. In all three bands, the high-luminosity AGN ($\log L_X > 44$) are formed before than the low-luminosity ones ($\log L_X < 44$), reaching the former a maximum in density at redshift $z \sim 1.5$ whereas the comoving density of the latter peak at $z \sim 0.7$.

References

1. Akiyama M., Ueda Y., Ohta K., et al., ApJS, 148, 275 (2003)
2. Barcons X., Carrera F.J., Ceballos M.T., et al., A&A, 476, 1191 (2007)
3. Caccianiga A., Severgnini P., Della Ceca R., et al., A&A, 477, 735 (2008)
4. Della Ceca R., Caccianiga A., Severgnini P., et al., A&A, 487, 119 (2008)
5. Giacconi R., Rosati P., Tozzi P., et al., ApJ, 551, 624 (2001)
6. Hasinger G., A&A, in press, astro-ph/0808.0260 (2008)
7. Hasinger G., Burg R., Giacconi R., et al., A&A, 329, 482 (1998)
8. Hasinger G., Miyaji T. & Schmidt M., A&A, 441, 417 (2005)
9. La Franca F., Fiore F., Comastri A., et al., ApJ, 635, 864 (2005)
10. Marshall H.L., Avni Y., Tananbaum H. & Zamorani G., ApJ, 269, 35 (1983)
11. Mason K.O., Carrera F.J., Hasinger G., et al., MNRAS, 311, 456 (2000)
12. Miyaji T., Hasinger G. & Schmidt M., A&A, 353, 25 (2000)
13. Schwope A.D., Hasinger G., Lehmann I., et al., AN, 321, 1 (200)
14. Silverman J.D., Green P.J., Barkhouse W.A., et al., ApJ, 679, 118 (2008)
15. Spergel D.N., Verde L., Peiris H.V., et al., ApJS, 148, 175 (2003)
16. Ueda Y., Akiyama M., Ohta K. & Miyaji T., ApJ, 598, 886 (2003)